Pergamon

Int. J. Solids Structures Vol. 35, No. 12, pp. 1219–1239, 1998

0020–7683/98 $19.00 + .00

PII: S0020–7683(97)00100–5

ANALYTICAL SOLUTION OF FINITE-GEOMETRY COMPOSITE PANELS UNDER TRANSIENT SURFACE LOADING

T. ANDERSON, E. MADENCI
Department of Aerospace and Mechanical Engineering, The University of Arizona, Aero. Building 16, Tucson, AZ 85721, U.S.A.

W. S. BURTON
Center for Computational Structures Technology, University of Virginia, Hampton, VA 23681, U.S.A.

and

J. C. FISH
Lockheed Martin Skunk Works, 1011 Lockheed Way, Palmdale, CA 93599, U.S.A.

(*Received* 14 *June* 1996; *in revised form* 10 *April* 1997)

Abstract—This study presents an analytical three-dimensional transient solution of a multi-layer specially orthotropic panel with finite geometry subjected to an arbitrarily distributed transverse loading. Governing equations derived from Reissner's functional are solved by applying Fourier or Laplace transformation in time and enforcing the continuity of traction and displacement components between the adjacent layers. Complex material constants are utilized to achieve material damping. The accuracy of the present analysis is established by considering a thin laminate under quasi-static and transient loading. The solution of the static analysis is compared with a known analytical solution, and the transient analysis is compared with a finite element analysis. The results concerning the transient response of a composite sandwich panel are also presented. Material damping is found to significantly affect the transient stress and displacement fields of a laminate, particularly for sandwich composite panels. © 1998 Elsevier Science Ltd.

1. INTRODUCTION

Understanding the impact damage characteristics of laminates and composite sandwich panels becomes imperative as their use increases in the construction of primary aircraft components. Sandwich panels are fabricated by bonding thin laminates (face sheets) on the outer surfaces of a lightweight shear-carrying honeycomb or foam core material. Both the laminate and sandwich panels are very susceptible to low-velocity (projectile velocity less than 150 ft/s) impacts such as dropped tools, runway stones, and tire blowout debris.

For solid laminates, visual examination of the impacted surface reveals very little damage because most of the degradation occurs internally near the back face sheet. With a sandwich panel, damage in the form of a shallow dent, visible near the impact area, is due to core crushing and delamination within the face sheet. Associated with the dent is a delamination at the interface between the face sheet and the core. The physical characteristics of internal damage caused by impact on composite laminates or sandwich panels can be found in Starnes and Williams (1984) and Nettles *et al.* (1990), respectively. Even at relatively low impact speeds, destructive and nondestructive evaluation methods indicate the primary damage mode involves interlaminar delaminations, resulting in a significant loss of bending stiffness.

Several mechanisms may participate in creating the local impact damage. Based on experimental investigations, Starnes and Williams (1984) observed that a transient compressive normal stress is initiated and propagates through the panel during the impact event, and that the compressive stress wave reflects from the back surface of the laminate as a tension wave and may produce matrix cracking. In the case of sandwich panels,

however, the strength of the tension wave is rather weak because the core absorbs the incoming compressive stress waves. Local transient bending waves are then initiated following several reflections of the transient normal waves. Interlaminar stresses associated with the local bending may cause damage or, if damage is present, this local bending deflection may cause the damage to propagate. Deformations due to the overall plate structural response, however, are initiated long after the transient bending and tension waves occur.

If the impact phenomenon is treated as a transient contact problem, the analysis is quite complex. In order to simplify it, Cairns and Lagace (1989), Olsson (1992), and Lee *et al.* (1993) decoupled the local contact effects from the global dynamic response of the plate. In these analyses, the effect of local contact between the indentor and the plate was invoked in the global dynamic analysis through the transient response of the plate coupled with the motion of the impactor. Coupling was achieved by modeling the contact behavior between the impactor and the panel by a spring, whose stiffness was obtained from experimental static indentation tests. Since the extent of the contact region and its force distribution were not known a priori, the contact behavior between the impactor and the panel was approximated by performing static indentation tests with spherical and cylindrical indentors. This assumption facilitated the use of static indentation laws for predicting the force deformation relationship produced by the impactor. These experimental investigations of the contact behavior, however, provide only the force-indentation relation, not the extent of the contact region and the force distribution. Also, analytical models, such as the one by Cairns and Lagace (1987), exist for predicting the force-indentation relation by assuming known contact stresses in the form of Hertzian-type pressure distributions.

For damage-tolerant design, accurate assessment of the stress and displacement fields is required for failure prediction of such components under transient surface loading. The presence of transverse shear deformation and the general material orthotropy coupled with transient surface loading, however, renders the analysis rather complex. In order to make the mathematical statement of the problem tractable, several approximate solution methods have been introduced. The Classical Laminate Theory (CLT), which accounts for the coupling effects of non-symmetric laminates, was examined by Pister and Dong (1959), Reissner and Stavsky (1961), and Dong *et al.* (1962). This approach cannot account for the through-the-thickness effects because it disregards the transverse normal and shear stresses. In addition, the validity of this approach is questionable when the material properties differ appreciably from layer to layer and/or when a high degree of anisotropy exists in one or more layers as discussed by Ambartsumyan (1962). Also, the uniform displacement assumption through the thickness of a cross section becomes invalid for panels subjected to concentrated dynamic loads on the surface. Therefore, CLT is not suitable for predicting interlaminar damage caused by impact. Although CLT suffers from these shortcomings, it provides reasonably accurate transverse deflections for thin laminates.

In order to improve the preceding approach, Chattopadhyay (1977), Whitney and Sun (1977), Dobyns (1981), Ramkumar and Chen (1983), and Lee *et al.* (1993) utilized Mindlin's (1951) plate theory to include the effect of transverse shear deformation. Although Mindlin's plate theory is a significant improvement over the CLT, it still suffers from an inability to determine the transverse normal stress. In addition, first-order shear deformation theory requires the transverse shear stiffness to be determined. The accuracy of the transverse shear stiffness depends upon a correction factor whose accurate determination is not easily achieved. An in-depth discussion on the determination of this parameter can be found in Noor and Burton (1990a). As with the CLT, this approach also assumes uniform displacement across the thickness, and it is suitable only for moderately thick laminates. For sandwich panels, the assumption of uniform transverse displacement is not valid because the core experiences local deformation near the impact region.

Although these investigations may provide adequately accurate results for thin plates under quasi-static loading, i.e., the time required to increase the magnitude of the applied load is longer than the period of the lowest vibration mode, their accuracy suffers if the loading rate is high, i.e., the time required to increase the magnitude of the applied load from zero to its maximum value is less than half the natural period of the structure.

Finite element analyses employing plate and shell elements based on the aforementioned plate theories also fail to predict the transient transverse normal stress in the panel. Using three-dimensional solid elements, Lee *et al.* (1984) and Wu and Springer (1988) modeled a laminate with several layers of elements per ply to capture the through-the-thickness effects. This type of analysis becomes computationally very intensive when modeling many layers. Consequently, a rigorous three-dimensional elasticity analysis is required to accurately determine the transient stress and displacement fields of a composite panel subjected to transverse impact.

An exact theory of elasticity was used by Mal and Lih (1992) and Lih and Mal (1995) to model the transient response of a unidirectional laminate subjected to concentrated and distributed surface loads. They constructed the solution for an infinite laminate by applying integral transformation techniques. A three-dimensional exact solution of a finite-geometry laminate with arbitrary stacking sequence subjected to a static transverse load was developed by Pagano (1970). Even though the analysis was for a static transverse load, the solution was still cumbersome, with different general solutions for specific laminate stacking sequences.

The present study provides a straightforward method to determine the transient solution of a multi-layer and finite-geometry panel under transverse loading. Each of the individual layers of the panel is modeled as an elastic, homogeneous, and specially orthotropic material. The finite-geometry panel is supported by rollers and is subjected to an arbitrarily distributed surface load. The governing equations derived from Reissner's functional (Reissner, 1950) are solved by applying the Fourier or Laplace transformation in time while enforcing the continuity of traction and displacement components between the adjacent layers. This analysis provides an efficient three-dimensional analytical solution for the stress and displacement fields under specified surface loading representations of the impact event.

2. PROBLEM STATEMENT

This study is concerned with the stress and displacement fields in a finite-geometry composite panel subjected to transient surface loading. The geometry and loading of the panel are illustrated in Fig. 1. A Cartesian reference coordinate system (x, y, z) is located at the corner on the upper surface of the panel. The length and width of the rectangular panel are denoted by a and b, and its thickness by h. In Fig. 2, the position of the interfaces in reference to the upper surface of the panel are specified by z^k. The thickness of the kth layer is given by $t^k = z^k - z^{k-1}$.

The panel is composed of layers made of homogeneous, elastic, and specially orthotropic materials. Each layer has elastic moduli E_L and E_T, shear modulus G_{LT}, and Poisson's ratios ν_{TL} and ν_{TZ} where the subscripts L, T, and Z are the longitudinal, transverse, and thickness directions relative to the fibers. When the material and reference coordinate systems coincide, the constitutive relationship for the kth layer is represented by

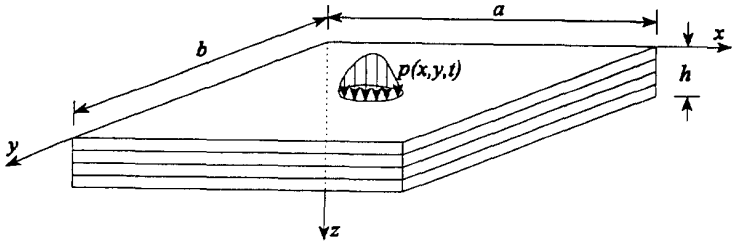

Fig. 1. Panel geometry and loading configuration.

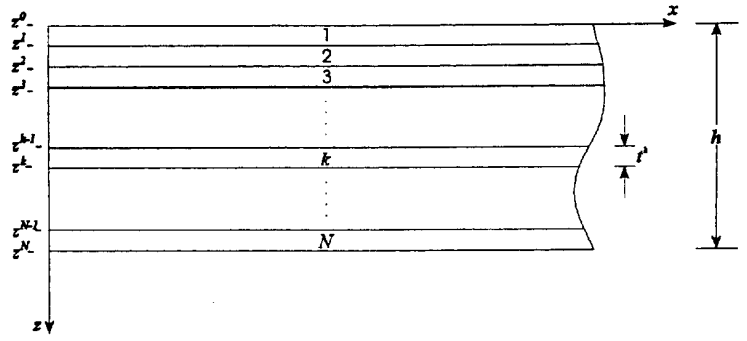

Fig. 2. Identification of the layers and their position in relation to the reference frame.

$$\begin{Bmatrix} \varepsilon_{xx} \\ \varepsilon_{yy} \\ \varepsilon_{zz} \\ \varepsilon_{yz} \\ \varepsilon_{zx} \\ \varepsilon_{xy} \end{Bmatrix}^k = \begin{bmatrix} D_{11} & D_{12} & D_{13} & 0 & 0 & 0 \\ D_{12} & D_{22} & D_{23} & 0 & 0 & 0 \\ D_{13} & D_{23} & D_{33} & 0 & 0 & 0 \\ 0 & 0 & 0 & D_{44} & 0 & 0 \\ 0 & 0 & 0 & 0 & D_{55} & 0 \\ 0 & 0 & 0 & 0 & 0 & D_{66} \end{bmatrix}^k \begin{Bmatrix} \sigma_{xx} \\ \sigma_{yy} \\ \sigma_{zz} \\ \sigma_{yz} \\ \sigma_{zx} \\ \sigma_{xy} \end{Bmatrix}^k \quad \text{or } \boldsymbol{\varepsilon}^k = \mathbf{D}^k \boldsymbol{\sigma}^k \tag{1}$$

where σ_{ij} and ε_{ij} are the components of the stress and strain tensors, respectively, and D_{ij} represent the compliance matrix with five independent constants. For balanced laminates for which the material and reference coordinate systems do not coincide, a method presented in the Appendix provides an average compliance matrix. This average compliance matrix will contain the nine independent coefficients of a specially orthotropic material.

As introduced by Mal and Lih (1992), the dissipation of energy due to material damping in composite panels is invoked in the analysis by allowing a small percentage of the compliance matrix to be complex. In general, the material damping is a function of the frequency; however, in this analysis, the complex compliance is assumed to be a constant value for all frequencies.

The boundary conditions along the edges of the panel are representative of roller supports. The edges are free to move in the x and y directions at $x = 0$ and $x = a$ and at $y = 0$ and $y = b$, respectively. The boundary conditions are expressed as

$$\begin{aligned} v^k = w^k = 0, \quad \sigma_{xx}^k = 0 \quad \text{for } x = 0, \quad x = a, \quad 0 \leqslant y \leqslant b \\ u^k = w^k = 0, \quad \sigma_{yy}^k = 0 \quad \text{for } y = 0, \quad y = b, \quad 0 \leqslant x \leqslant a \end{aligned} \tag{2}$$

where u, v and w represent the displacement components in the x, y, and z directions, respectively.

The layers in the panel are treated as perfectly bonded with continuous tractions and displacements across the layer interfaces. Continuity of traction and displacement components is imposed

$$\sigma_{\alpha z}^k|_{z=z^k} - \sigma_{\alpha z}^{k+1}|_{z=z^k} = 0 \quad \alpha = x, y, z \tag{3}$$

and

$$\left.\begin{aligned} u^k|_{z=z^k} - u^{k+1}|_{z=z^k} &= 0 \\ v^k|_{z=z^k} - v^{k+1}|_{z=z^k} &= 0 \\ w^k|_{z=z^k} - w^{k+1}|_{z=z^k} &= 0 \end{aligned}\right\} \quad k = 1, \ldots, N-1. \tag{4}$$

The $z = z^{(0)}$ surface of the panel is subjected to an arbitrary distributed load, and the $z = z^N$ surface is free of tractions. These surface tractions are enforced as

$$\begin{aligned} \sigma^N_{\alpha z}|_{z=z^N} &= 0 \quad \alpha = x, y, z \\ \sigma^1_{\alpha z}|_{z=z^0} &= 0 \quad \alpha = x, y \\ \sigma^1_{zz}|_{z=z^0} &= p(x, y, t) \end{aligned} \tag{5}$$

where $p(x, y, t)$ represents the external transverse distributed load.

3. SOLUTION METHOD

In this study, the governing equations are derived by applying variational principles to Reissner's functional (Reissner, 1950), Π_R given in the form

$$\Pi_R = \int_V (\boldsymbol{\sigma}^T \boldsymbol{\varepsilon} - \tfrac{1}{2}\boldsymbol{\sigma}^T \mathbf{D} \boldsymbol{\sigma} - \mathbf{B}^T \mathbf{u})\, dV - \int_{S_1} \mathbf{T}^T \mathbf{u}\, dS \tag{6}$$

in which **B**, **T**, and **u** are the vectors of body force, traction, and displacement components, and S_1 is the surface of the body over which the tractions are applied. In expressing the strain energy and potential of the applied loads, Reissner's functional treats both the stress and displacement components as dependent variables. For a transient analysis, the body force vector **B** consists of the components of the inertial force

$$\mathbf{B}^T = \left[-\rho \frac{\partial^2 u}{\partial t^2}, \quad -\rho \frac{\partial^2 v}{\partial t^2}, \quad -\rho \frac{\partial^2 w}{\partial t^2} \right] \tag{7}$$

with ρ being the density.

Applying the variational principles, the stress and displacement components over the volume of a body yield the governing Euler–Lagrange equations utilized previously by Noor and Burton (1990b). The time dependency in the equations is removed by applying either a Fourier transformation

$$\hat{f}(w) = \int_{-\infty}^{\infty} f(t)\, e^{i\omega t}\, dt \tag{8}$$

or a Laplace transformation

$$\hat{f}(s) = \int_0^{\infty} f(t)\, e^{-st}\, dt \tag{9}$$

where ω and s are the transformation variables and $i = \sqrt{-1}$. Material damping introduced in the form of a complex compliance

$$\bar{\mathbf{D}} = \mathbf{D} + i\varepsilon \mathbf{D} \tag{10}$$

with a small parameter ε, ensures that the integrand in the Fourier transformation vanishes as time proceeds. Because the integrand in the Laplace transformation converges with time,

the compliance matrix can be treated as real or complex for Laplace transformation. In the Fourier or Laplace domain, the transformed governing equations with complex compliance become

$$\bar{D}^k_{11}\hat{\sigma}^k_{xx}+\bar{D}^k_{12}\hat{\sigma}^k_{yy}+\bar{D}^k_{13}\hat{\sigma}^k_{zz}-\frac{\partial\hat{u}^k}{\partial x}=0 \tag{11}$$

$$\bar{D}^k_{12}\hat{\sigma}^k_{xx}+\bar{D}^k_{22}\hat{\sigma}^k_{yy}+\bar{D}^k_{23}\hat{\sigma}^k_{zz}-\frac{\partial\hat{v}^k}{\partial y}=0 \tag{12}$$

$$\bar{D}^k_{13}\hat{\sigma}^k_{xx}+\bar{D}^k_{23}\hat{\sigma}^k_{yy}+\bar{D}^k_{33}\hat{\sigma}^k_{zz}-\frac{\partial\hat{w}^k}{\partial z}=0 \tag{13}$$

$$\bar{D}^k_{44}\hat{\sigma}^k_{yz}-\frac{\partial\hat{v}^k}{\partial z}-\frac{\partial\hat{w}^k}{\partial y}=0 \tag{14}$$

$$\bar{D}^k_{55}\hat{\sigma}^k_{zx}-\frac{\partial\hat{u}^k}{\partial z}-\frac{\partial\hat{w}^k}{\partial x}=0 \tag{15}$$

$$\bar{D}^k_{66}\hat{\sigma}^k_{xy}-\frac{\partial\hat{u}^k}{\partial y}-\frac{\partial\hat{v}^k}{\partial x}=0 \tag{16}$$

$$\frac{\partial\hat{\sigma}^k_{xx}}{\partial x}+\frac{\partial\hat{\sigma}^k_{xy}}{\partial y}+\frac{\partial\hat{\sigma}^k_{zx}}{\partial z}+\gamma^2\rho^k\hat{u}^k=0 \tag{17}$$

$$\frac{\partial\hat{\sigma}^k_{xy}}{\partial x}+\frac{\partial\hat{\sigma}^k_{yy}}{\partial y}+\frac{\partial\hat{\sigma}^k_{yz}}{\partial z}+\gamma^2\rho^k\hat{v}^k=0 \tag{18}$$

$$\frac{\partial\hat{\sigma}^k_{zx}}{\partial x}+\frac{\partial\hat{\sigma}^k_{yz}}{\partial y}+\frac{\partial\hat{\sigma}^k_{z}}{\partial z}+\gamma^2\rho^k\hat{w}^k=0 \tag{19}$$

in which the symbol "^" denotes the transformed variables and the transformation variable γ is defined as

$$\gamma^2=\omega^2=-s^2. \tag{20}$$

These governing equations are reduced to a system of ordinary differential equations by representing the stress and displacement components for the kth layer in terms of Fourier series in which $\hat{\sigma}_{xxmn}$, $\hat{\sigma}_{yymn}$, ..., $\hat{w}_{mn}$ are unknown auxiliary functions for each m and n and $\alpha_m=m\pi/a$ and $\beta_n=n\pi/b$. Substituting for the stress and displacement components in terms of their Fourier series in the governing equations leads to

$$\sum_{m=1}^{\infty}\sum_{n=1}^{\infty}[\bar{D}^k_{11}\hat{\sigma}^k_{xxmn}+\bar{D}^k_{12}\hat{\sigma}^k_{yymn}+\bar{D}^k_{13}\hat{\sigma}^k_{zzmn}+\hat{u}^k_{mn}\alpha_m]\sin\alpha_m x\sin\beta_n y=0 \tag{21}$$

$$\sum_{m=1}^{\infty}\sum_{n=1}^{\infty}[\bar{D}^k_{12}\hat{\sigma}^k_{xxmn}+\bar{D}^k_{22}\hat{\sigma}^k_{yymn}+\bar{D}^k_{23}\hat{\sigma}^k_{zzmn}+\hat{v}^k_{mn}\beta_n]\sin\alpha_m x\sin\beta_n y=0 \tag{22}$$

$$\sum_{m=1}^{\infty}\sum_{n=1}^{\infty}\left[\bar{D}^k_{13}\hat{\sigma}^k_{xxmn}+\bar{D}^k_{23}\hat{\sigma}^k_{yymn}+\bar{D}^k_{33}\hat{\sigma}^k_{zzmn}+\frac{\partial\hat{w}^k_{mn}}{\partial z}\right]\sin\alpha_m x\sin\beta_n y=0 \tag{23}$$

$$\sum_{m=1}^{\infty}\sum_{n=1}^{\infty}\left[\bar{D}_{44}^{k}\hat{\sigma}_{yzmn}^{k}-\frac{\partial\hat{v}_{mn}^{k}}{\partial z}-\hat{w}_{mn}^{k}\beta_m\right]\sin\alpha_m x\cos\beta_n y=0 \tag{24}$$

$$\sum_{m=1}^{\infty}\sum_{n=1}^{\infty}\left[\bar{D}_{55}^{k}\hat{\sigma}_{zxmn}^{k}-\frac{\partial\hat{u}_{mn}^{k}}{\partial z}-\hat{w}_{mn}^{k}\alpha_m\right]\cos\alpha_m x\sin\beta_n y=0 \tag{25}$$

$$\sum_{m=1}^{\infty}\sum_{n=1}^{\infty}[\bar{D}_{66}^{k}\hat{\sigma}_{xymn}^{k}-\hat{u}_{mn}^{k}\beta_n-\hat{w}_{mn}^{k}\alpha_m]\cos\alpha_m x\cos\beta_n y=0 \tag{26}$$

$$\sum_{m=1}^{\infty}\sum_{n=1}^{\infty}\left[\rho^{k}\gamma^{2}\hat{u}_{mn}^{k}+\hat{\sigma}_{xxmn}^{k}\alpha_m-\hat{\sigma}_{xymn}^{k}\beta_n+\frac{\partial\hat{\sigma}_{zxmn}^{k}}{\partial z}\right]\cos\alpha_m x\sin\beta_n y=0 \tag{27}$$

$$\sum_{m=1}^{\infty}\sum_{n=1}^{\infty}\left[\rho^{k}\gamma^{2}\hat{v}_{mn}^{k}-\hat{\sigma}_{xymn}^{k}\alpha_m+\hat{\sigma}_{yymn}^{k}\beta_n+\frac{\partial\hat{\sigma}_{yzmn}^{k}}{\partial z}\right]\sin\alpha_m x\cos\beta_n y=0 \tag{28}$$

$$\sum_{m=1}^{\infty}\sum_{n=1}^{\infty}\left[\rho^{k}\gamma^{2}\hat{w}_{mn}^{k}-\hat{\sigma}_{zxmn}^{k}\alpha_m-\hat{\sigma}_{yzmn}^{k}\beta_n+\frac{\partial\hat{\sigma}_{zzmn}^{k}}{\partial z}\right]\sin\alpha_m x\sin\beta_n y=0. \tag{29}$$

The Fourier series representation of the loading function in terms of the transformation variables becomes

$$\hat{p}(x,y,\gamma)=\sum_{m=1}^{\infty}\sum_{n=1}^{\infty}\hat{p}_{mn}(\gamma)\sin\alpha_m x\sin\beta_n y \tag{30}$$

with the Fourier series coefficient expressed as

$$\hat{p}_{mn}(\gamma)=\frac{4}{ab}\int_a^b\int_a^b\hat{p}(x,y,\gamma)\sin\alpha_m x\sin\beta_n y\,\mathrm{d}x\,\mathrm{d}y. \tag{31}$$

The resulting ordinary differential equations corresponding to a specific m and n can be expressed in matrix form as

$$\begin{bmatrix}\mathbf{M}_{11} & \mathbf{M}_{12}\\ \mathbf{M}_{21} & \mathbf{M}_{22}\end{bmatrix}^{k}\begin{Bmatrix}\mathbf{F}\\ \mathbf{S}\end{Bmatrix}^{k}+\begin{bmatrix}0 & 0\\ 0 & \mathbf{N}_{22}\end{bmatrix}^{k}\begin{Bmatrix}\dfrac{\partial\mathbf{F}}{\partial z}\\ \dfrac{\partial\mathbf{S}}{\partial z}\end{Bmatrix}^{k}=\begin{Bmatrix}0\\ 0\end{Bmatrix} \tag{32}$$

where $\mathbf{F}^{\mathrm{T}}=\{\hat{\sigma}_{xxmn},\hat{\sigma}_{yymn},\hat{\sigma}_{xymn}\}$ and $\mathbf{S}^{\mathrm{T}}=\{\hat{\sigma}_{yzmn},\hat{\sigma}_{zxmn},\hat{\sigma}_{zzmn},\hat{u}_{mn},\hat{v}_{mn},\hat{w}_{mn}\}$. The explicit forms of $\mathbf{M}_{11}$, $\mathbf{M}_{12}$, $\mathbf{M}_{21}$, and $\mathbf{M}_{22}$ are given by

$$\mathbf{M}_{11}^{k}=\begin{bmatrix}\bar{D}_{11} & \bar{D}_{12} & 0\\ \bar{D}_{12} & \bar{D}_{22} & 0\\ 0 & 0 & \bar{D}_{66}\end{bmatrix}^{k},\quad \mathbf{M}_{12}^{k}=\mathbf{M}_{21}^{k^{\mathrm{T}}}=\begin{bmatrix}0 & 0 & \bar{D}_{13} & \alpha_m & 0 & 0\\ 0 & 0 & \bar{D}_{23} & 0 & \beta_n & 0\\ 0 & 0 & 0 & -\beta_n & -\alpha_m & 0\end{bmatrix}^{k}$$

and

$$\mathbf{M}_{22}^k = \begin{bmatrix} \bar{D}_{44} & 0 & 0 & 0 & 0 & -\beta_n \\ 0 & \bar{D}_{55} & 0 & 0 & 0 & -\alpha_m \\ 0 & 0 & \bar{D}_{33} & 0 & 0 & 0 \\ 0 & 0 & 0 & \gamma^2\rho & 0 & 0 \\ 0 & 0 & 0 & 0 & \gamma^2\rho & 0 \\ -\beta_n & -\alpha_m & 0 & 0 & 0 & \gamma^2\rho \end{bmatrix}, \quad \mathbf{N}_{22}^k = \begin{bmatrix} 0 & 0 & 0 & 0 & -1 & 0 \\ 0 & 0 & 0 & -1 & 0 & 0 \\ 0 & 0 & 0 & 0 & 0 & -1 \\ 0 & 1 & 0 & 0 & 0 & 0 \\ 1 & 0 & 0 & 0 & 0 & 0 \\ 0 & 0 & 1 & 0 & 0 & 0 \end{bmatrix}.$$

The matrix representation of the governing differential equations permits the expression of the vector $\mathbf{F}^k$ (containing the in-plane stress coefficients) in terms of the vector $\mathbf{S}^k$ (containing the displacement and out-of-plane stress coefficients) as

$$\mathbf{F}^k = -\mathbf{M}_{11}^{k^{-1}}\mathbf{M}_{12}^k\mathbf{S}^k. \tag{33}$$

Substituting for $\mathbf{F}^k$ in eqn (32) results in a coupled system of first-order ordinary differential equations

$$\frac{\partial \mathbf{S}^k}{\partial z} + \mathbf{K}^k\mathbf{S}^k = 0 \tag{34}$$

with

$$\mathbf{K}^k = \mathbf{N}_{22}^{k^{-1}}[-\mathbf{M}_{12}^{k^{\mathrm{T}}}\mathbf{M}_{11}^{k^{-1}}\mathbf{M}_{12}^k + \mathbf{M}_{22}^k]. \tag{35}$$

The solution to the homogeneous system of equations is readily constructed by assuming

$$\mathbf{S}^k = \mathbf{C}^k e^{-\lambda^k z}. \tag{36}$$

In constructing the solution, the determinant of the system of equations must vanish in order for a non-trivial solution to exist. The characteristic equation for the kth layer takes the form

$$(\lambda^k)^6 + L^k(\lambda^k)^4 + M^k(\lambda^k)^2 + N^k = 0 \tag{37}$$

with L^k, M^k, and N^k expressed in terms of the components of $\mathbf{K}^k$. This form of the characteristic equation reveals that three of the roots (eigenvalues) are the opposite sign of the remaining ones: λ_1^k, λ_2^k, λ_3^k and $-\lambda_1^k$, $-\lambda_2^k$, $-\lambda_3^k$. The coupled system of equations can be decoupled by allowing

$$\mathbf{S}^k = \mathbf{Q}^k\mathbf{R}^k \tag{38}$$

where $\mathbf{Q}^k$ is the transformation matrix of eigenvectors.

The decoupled system of equations becomes

$$\frac{\partial \mathbf{R}^k}{\partial z} + \Lambda^k\mathbf{R}^k = 0 \tag{39}$$

in which Λ^k is a diagonal matrix composed of the eigenvalues. By the procedure developed by Mal (1988), the solution to the decoupled system of equations is written as

$$\mathbf{R}^k(z) = \mathbf{E}^k(z)\mathbf{C}^k = \begin{bmatrix} e^{-\lambda_1 z} & 0 & 0 & 0 & 0 & 0 \\ 0 & e^{-\lambda_2 z} & 0 & 0 & 0 & 0 \\ 0 & 0 & e^{-\lambda_3 z} & 0 & 0 & 0 \\ 0 & 0 & 0 & e^{\lambda_1 z} & 0 & 0 \\ 0 & 0 & 0 & 0 & e^{\lambda_2 z} & 0 \\ 0 & 0 & 0 & 0 & 0 & e^{\lambda_3 z} \end{bmatrix}^k \begin{Bmatrix} C_1 \\ C_2 \\ C_3 \\ C_4 \\ C_5 \\ C_6 \end{Bmatrix}^k. \tag{40}$$

Using the transformation matrix, $\mathbf{Q}^k$, the solution for the out-of-plane stress and displacement coefficients becomes

$$\mathbf{S}^k(z) = \mathbf{Q}^k\mathbf{E}^k(z)\mathbf{C}^k. \tag{41}$$

Prior to enforcing the boundary and continuity conditions so as to determine the constants $\mathbf{C}^k$ for each layer, the matrix $\mathbf{E}^k$ is multiplied by a vector of constants (the first and second three rows by $e^{\lambda_i z^k}$ and $e^{-\lambda_i z^{k-1}}$, respectively) so that it takes a suitable form with negative exponents in the formulation of layered systems:

$$\mathbf{E}^k(z) = \begin{bmatrix} e^{\lambda_1^k(z^k - z)} & 0 & 0 & 0 & 0 & 0 \\ 0 & e^{\lambda_2^k(z^k - z)} & 0 & 0 & 0 & 0 \\ 0 & 0 & e^{\lambda_3^k(z^k - z)} & 0 & 0 & 0 \\ 0 & 0 & 0 & e^{\lambda_1^k(z - z^{k-1})} & 0 & 0 \\ 0 & 0 & 0 & 0 & e^{\lambda_2^k(z - z^{k-1})} & 0 \\ 0 & 0 & 0 & 0 & 0 & e^{\lambda_3^k(z - z^{k-1})} \end{bmatrix}. \tag{42}$$

In the case of the kth layer, the matrix $\mathbf{E}^k$ is evaluated at the $k-1$ interface as

$$\mathbf{E}^k(z^{k-1}) = \begin{bmatrix} \mathbf{E}_t & 0 \\ 0 & \mathbf{I} \end{bmatrix}^k \tag{43}$$

where $\mathbf{I}$ is a 3×3 identity matrix and

$$\mathbf{E}_t^k = \begin{bmatrix} e^{\lambda_1 t} & 0 & 0 \\ 0 & e^{\lambda_2 t} & 0 \\ 0 & 0 & e^{\lambda_3 t} \end{bmatrix}^k \tag{44}$$

with t^k equal to the thickness of the kth layer. Similarly, for the interface of the kth layer,

$$\mathbf{E}^k(z^k) = \begin{bmatrix} \mathbf{I} & 0 \\ 0 & \mathbf{E}_t \end{bmatrix}^k. \tag{45}$$

Decomposing the vector $\mathbf{S}^k$ in the form

$$\mathbf{S}^k(z) = \begin{Bmatrix} \mathbf{T}(z) \\ \mathbf{U}(z) \end{Bmatrix}^k \tag{46}$$

with

$$\mathbf{T}^{k^T} = [\hat{\sigma}_{yzmn} \quad \hat{\sigma}_{zxmn} \quad \hat{\sigma}_{zzmn}] \tag{47}$$

and

$$\mathbf{U}^{k^T} = [\hat{u}_{mn} \quad \hat{v}_{mn} \quad \hat{w}_{mn}] \tag{48}$$

permits the equations for the stress and displacement coefficients at the $k-1$ and k interfaces to be rewritten as

$$\begin{Bmatrix} \mathbf{T}(z^{k-1}) \\ \mathbf{U}(z^{k-1}) \end{Bmatrix}^k = \begin{bmatrix} \mathbf{Q}_{11} & \mathbf{Q}_{12} \\ \mathbf{Q}_{21} & \mathbf{Q}_{22} \end{bmatrix}^k \begin{bmatrix} \mathbf{E}_t & 0 \\ 0 & \mathbf{I} \end{bmatrix}^k \begin{Bmatrix} \mathbf{C}_+ \\ \mathbf{C}_- \end{Bmatrix}^k \tag{49}$$

and

$$\begin{Bmatrix} \mathbf{T}(z^k) \\ \mathbf{U}(z^k) \end{Bmatrix}^k = \begin{bmatrix} \mathbf{Q}_{11} & \mathbf{Q}_{12} \\ \mathbf{Q}_{21} & \mathbf{Q}_{22} \end{bmatrix}^k \begin{bmatrix} \mathbf{I} & 0 \\ 0 & \mathbf{E}_t \end{bmatrix}^k \begin{Bmatrix} \mathbf{C}_+ \\ \mathbf{C}_- \end{Bmatrix}^k \tag{50}$$

respectively, where $\mathbf{Q}_{ij}$ are the submatrices of the transformation matrix $\mathbf{Q}$. The vectors $\mathbf{C}_+^k$ and $\mathbf{C}_-^k$ contain the unknown coefficients consistent with the partitioning of the matrix $\mathbf{Q}^k$ for each layer.

The boundary conditions at $z = z^0$ and $z = z^N$ surfaces can be expressed as

$$\mathbf{T}^1(z^0) = \begin{Bmatrix} 0 \\ 0 \\ \hat{P}_{mn} \end{Bmatrix} = \mathbf{Q}_{11}^1 \mathbf{E}_t^1 \mathbf{C}_+^1 + \mathbf{Q}_{12}^1 \mathbf{C}_-^1 \tag{51}$$

and

$$\mathbf{T}^N(z^N) = \begin{Bmatrix} 0 \\ 0 \\ 0 \end{Bmatrix} = \mathbf{Q}_{11}^N \mathbf{C}_+^N + \mathbf{Q}_{12}^N \mathbf{E}_t^N \mathbf{C}_-^N, \tag{52}$$

respectively. A recursive relationship is then established to enforce the continuity of out-of-plane stresses and displacements between the k and $k+1$ interfaces as

$$\mathbf{Q}_{11}^k \mathbf{C}_+^k + \mathbf{Q}_{12}^k \mathbf{E}_t^k \mathbf{C}_-^k - \mathbf{Q}_{11}^{k+1} \mathbf{E}_t^{k+1} \mathbf{C}_+^{k+1} - \mathbf{Q}_{12}^{k+1} \mathbf{C}_-^{k+1} = 0 \tag{53}$$

$$\mathbf{Q}_{21}^k \mathbf{C}_+^k + \mathbf{Q}_{22}^k \mathbf{E}_t^k \mathbf{C}_-^k - \mathbf{Q}_{21}^{k+1} \mathbf{E}_t^{k+1} \mathbf{C}_+^{k+1} - \mathbf{Q}_{22}^{k+1} \mathbf{C}_-^{k+1} = 0. \tag{54}$$

The boundary and continuity conditions are then rewritten in eqn (55) to form the algebraic equations to determine the unknown layer coefficients $\mathbf{C}_+^k$ and $\mathbf{C}_-^k$

$$\begin{bmatrix} \mathbf{Q}_{11}^1\mathbf{E}_t^1 & \mathbf{Q}_{12}^1 & 0 & 0 & & & & \\ \mathbf{Q}_{11}^1 & \mathbf{Q}_{12}^1\mathbf{E}_t^1 & -\mathbf{Q}_{11}^2\mathbf{E}_t^2 & -\mathbf{Q}_{12}^2 & & & & \\ \mathbf{Q}_{21}^1 & \mathbf{Q}_{22}^1\mathbf{E}_t^1 & -\mathbf{Q}_{21}^2\mathbf{E}_t^2 & -\mathbf{Q}_{22}^2 & & & & \\ & & \ddots & \ddots & \ddots & & & \\ & & & & \mathbf{Q}_{11}^{N-1} & \mathbf{Q}_{12}^{N-1}\mathbf{E}_t^{N-1} & -\mathbf{Q}_{11}^N\mathbf{E}_t^N & -\mathbf{Q}_{12}^N \\ & & & & \mathbf{Q}_{21}^{N-1} & \mathbf{Q}_{22}^{N-1}\mathbf{E}_t^{N-1} & -\mathbf{Q}_{21}^N\mathbf{E}_t^N & -\mathbf{Q}_{22}^N \\ & & & & 0 & 0 & \mathbf{Q}_{11}^N & \mathbf{Q}_{12}^N\mathbf{E}_t^N \end{bmatrix} \begin{Bmatrix} \mathbf{C}_+^1 \\ \mathbf{C}_-^1 \\ \mathbf{C}_+^2 \\ \mathbf{C}_-^2 \\ \vdots \\ \mathbf{C}_+^{N-1} \\ \mathbf{C}_-^{N-1} \\ \mathbf{C}_+^N \\ \mathbf{C}_-^N \end{Bmatrix}$$

$$= \begin{Bmatrix} \mathbf{T}^1(z^0) \\ 0 \\ 0 \\ 0 \\ \vdots \\ 0 \\ 0 \\ 0 \\ 0 \end{Bmatrix}. \quad (55)$$

The solution to this system of algebraic equations leads to the out-of-plane stress and displacement coefficients through the substitution of $\mathbf{C}^k$ into eqn (41). The in-plane stress coefficients are then obtained by eqn (33). The process of determining the stress and displacement coefficients is repeated for each value of m and n in the Fourier series representation.

The stress and displacement components determined as a function of the transformation variable are then transformed back to the time domain through Fourier or Laplace inversion integrals.

4. NUMERICAL RESULTS

A quasi-static response of a laminate is considered in order to validate the present analysis with the analytical solution given by Pagano (1970). After validating the present analysis, two transient analyses are performed to investigate the response of a thin laminate and a sandwich panel. The solution concerning the thin laminate is compared with that of a finite element analysis. The transient response of a sandwich panel with an absorptive core is examined for two damping parameters. The face sheets are free of damping. The results in the time domain are obtained by performing numerical inversions of Fourier or Laplace transformations.

Static analysis of a thick laminate

In order to verify the present analysis, a statically loaded rectangular panel is considered and the results are compared with the well-known analytical solution by Pagano (1970). The static sinusoidal loading is prescribed by the function

$$p(x, y) = \sigma \sin\frac{\pi}{a}x \sin\frac{\pi}{b}y \quad (56)$$

where σ is the amplitude of the loading. The plate is of length a in the x-direction and of width $b = 3a$ in the y-direction. The span-to-thickness ratio, $s(s = a/h)$, is equal to 4.

Table 1. Normalized solutions for Pagano (1970), CLT, and the present analysis

Normalized stress and displacement	Pagano (1970) 3-D elasticity solution	Pagano (1970) CLT	Present analysis
$\sigma^*_{xx}(a/2, b/2, 0)$	1.14	0.623	1.14
$\sigma^*_{xx}(a/2, b/2, h)$	−1.10	−0.623	−1.10
$\sigma^*_{yy}(a/2, b/2, h/3)$	0.109	0.0252	0.108
$\sigma^*_{zx}(0, b/2, h/2)$	0.351	0.440	0.351
$\sigma^*_{yz}(a/2, 0, h/2)$	0.0334	0.0108	0.0327
$\sigma^*_{xy}(0, 0, 0)$	−0.0269	−0.0083	−0.0268
$\sigma^*_{xy}(0, 0, h)$	0.0281	0.0083	0.0282
$w^*(a/2, b/2, h/2)$	2.82	0.503	2.82

The material coefficients used in the analysis are the same as those used by Pagano (1970) and given by

$$E_L = 25.0 \times 10^6 \text{ psi}$$
$$E_T = 1.0 \times 10^6 \text{ psi}$$
$$G_{LT} = 0.5 \times 10^6 \text{ psi}$$
$$G_{TZ} = 0.2 \times 10^6 \text{ psi}$$
$$\nu_{LT} = \nu_{TZ} = 0.25 \tag{57}$$

with a panel lay-up of [0°/90°/0°]. It is worth noting that this material is not transversely isotropic.

A simple modification to the present formulation is required to determine the static solution. This is achieved by setting the body force terms in Reissner's functional equal to zero. It is identical to solving the transient analysis with the transformation variable equal to zero.

For direct comparison with the results provided by Pagano (1970), the stress and displacement components are normalized as

$$[\sigma^*_{xx}, \sigma^*_{yy}, \sigma^*_{xy}] = \frac{1}{\sigma s^2}[\sigma_{xx}, \sigma_{yy}, \sigma_{xy}]$$
$$[\sigma^*_{zx}, \sigma^*_{yz}] = \frac{1}{\sigma s}[\sigma_{zx}, \sigma_{yz}]$$
$$w^* = \frac{100 E_T w}{\sigma h s^4}. \tag{58}$$

A comparison of the results is presented in Table 1. Excellent agreement is found between Pagano's three-dimensional elasticity solution and the present analysis. For reasons previously discussed, the solution provided by CLT was expected and does differ greatly from the solutions provided by Pagano and the present analysis.

Transient analysis of a thin laminate

A transient analysis is performed on a thin, square laminate with length and thickness equal to 10 inches and 0.25 inch, respectively. The laminate consists of 3 layers of equal thickness with a lay-up of [0°/90°/0°]. The material properties are the same as those given by Pagano (1970) and the density of the material is 2.5×10^{-4} slugs/in^3.

The panel is subjected to a non-uniform distributed load applied over a square region at the center. The loading is represented by $p(x, y, t) = g(x, y)h(t)$, where

$$g(x,y) = -(x-4)^2(x-6)^2(y-4)^2(y-6)^2; \quad 4 \leqslant x \leqslant 6, \quad 4 \leqslant y \leqslant 6 \tag{59}$$

and

$$h(t) = \begin{cases} 1; & t \leqslant 0.001 \text{ s} \\ 0; & t > 0.001 \text{ s} \end{cases}. \tag{60}$$

The function $g(x, y)$ is approximated by 15 terms in the Fourier series representation.

An inverse fast Fourier transform is performed at 16,384 points between 0 and 1 second. The damping parameter, ε, ensuring the integrand in eqn (8) to be convergent, is taken as 0.025. Although the period just subsequent to the impact is of interest, a 1-second time period is required to allow the panel's vibrations to attenuate. Upon completion, only the time period up to 0.0015 second is examined, as shown in Figs 3–8.

In order to capture the influence of the damping parameter, the results are compared with those obtained by applying the Laplace transformation and the finite element method. The numerical inversion routine utilized for Laplace transformation does not converge efficiently for all functions. Therefore, only the displacement at a point will be examined and compared with the results obtained from the Fourier transformation and the finite element analysis. The inverse FFT calculation proves to be a more efficient method for the other stress and displacement components.

In the finite element analysis conducted by using ABAQUS (Pawtucket, RI) the square plate is modeled with a 20×20 element mesh. The elements utilized in the analysis are of ABAQUS type S8R. These elements are eight-node shell elements with reduced integration. Although these shell elements are developed from the classical plate theory, they are intended to model thick panels, where estimates of the interlaminar shear stresses are required. Unlike the in-plane stresses, the transverse shear stresses are not calculated from the constitutive behavior of the shell. Instead, subsequent to the analysis, the ABAQUS finite element program estimates the transverse shear stresses based on a piecewise quadratic variation of the transverse shear stress across the section, under pure bending about one axis. These elements are still, however, incapable of determining the transverse normal stress.

A comparison of the finite element results with those determined by the present analysis are presented in Figs 3–8. Excellent agreement is found for the transverse displacement

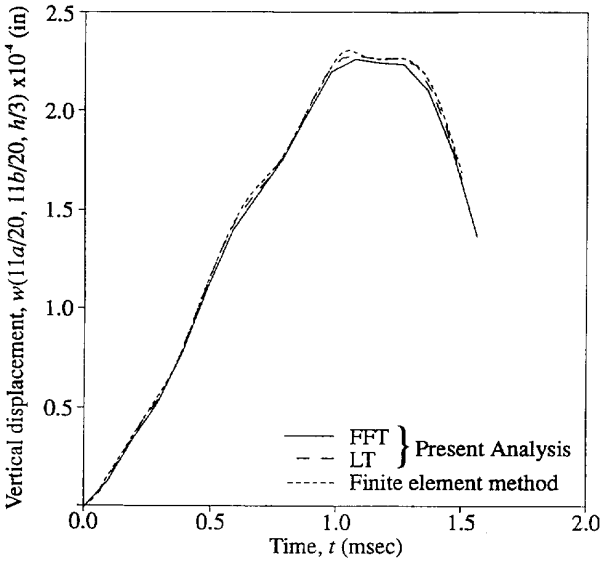

Fig. 3. Variation of vertical displacement, w, as a function of time for the thin laminate at $x = 11a/20$, $y = 11b/20$, and $z = h/3$.

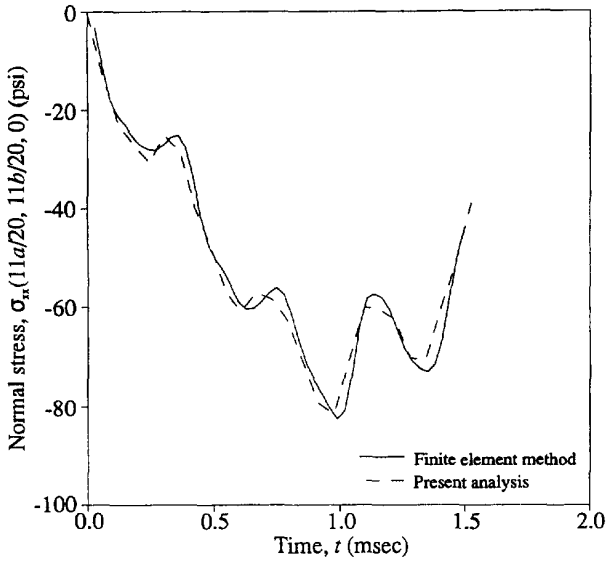

Fig. 4. Variation of normal stress, σ_{xx}, as a function of time for the thin laminate at $x = a/20$, $y = 11b/20$, and $z = 0$.

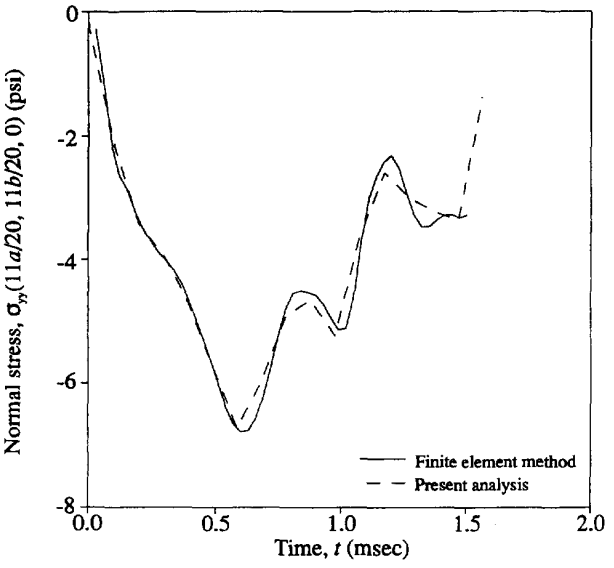

Fig. 5. Variation of normal stress, σ_{yy}, as a function of time for the thin laminate at $x = a/20$, $y = 11b/20$, and $z = 0$.

between the three solution methods, suggesting the small damping parameter included in the Fourier transformation formulation has relatively little effect shortly after the impact event. Close agreement is also observed between the ABAQUS solutions and Fourier transformation solutions for the in-plane and transverse and shear stresses.

Transient analysis of a sandwich panel

A sandwich panel with elastic face sheets without damping and an absorptive core with damping is subjected to transverse impact. The panel is composed of layers with a stacking sequence of [0°/90°/core/90°/0°]. The material properties of the elastic face sheets are the same as those used by Pagano (1970). The transversely isotropic material properties of the core are

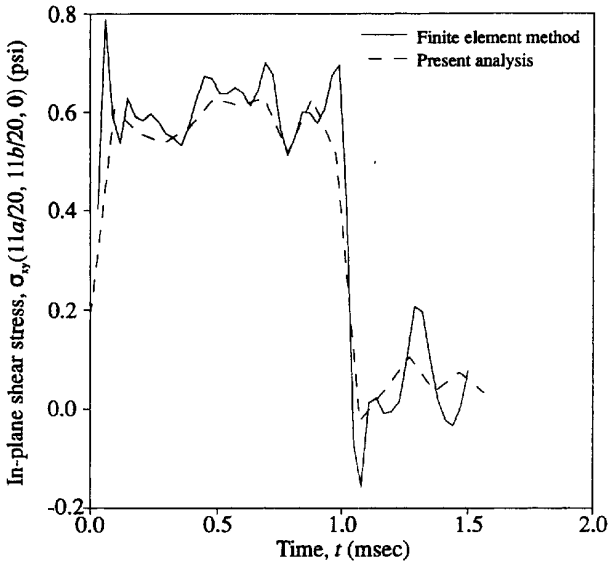

Fig. 6. Variation of in-plane shear stress, σ_{xy}, as a function of time for the thin laminate at $x = 11a/20$, $y = 11b/20$, and $z = 0$.

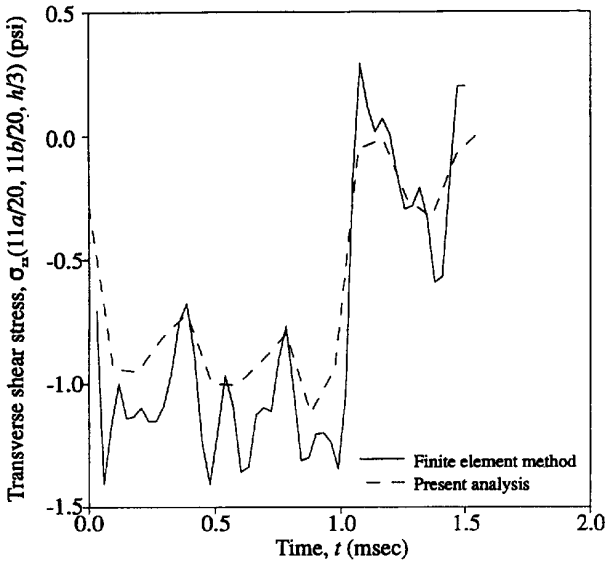

Fig. 7. Variation of transverse shear stress, σ_{xz}, as a function of time for the thin laminate at $x = 11a/20$, $y = 11b/20$, and $z = h/3$.

$$E_{TZ} = 0.04 \times 10^6 \text{ psi}$$
$$E_{LL} = 0.5 \times 10^6 \text{ psi}$$
$$G_{LT} = 0.06 \times 10^6 \text{ psi}$$
$$\nu_{TZ} = \nu_{TL} = 0.25 \tag{61}$$

and the density of the core is 5.4×10^{-5} slugs/in^3 (3 lbs/ft^3). The panel is 10 inches square and the thickness of the plies and core are 0.02 and 0.5 inch, respectively. The panel is subjected to the loading distribution $p(x, y, t) = g(x, y)h(t)$, where

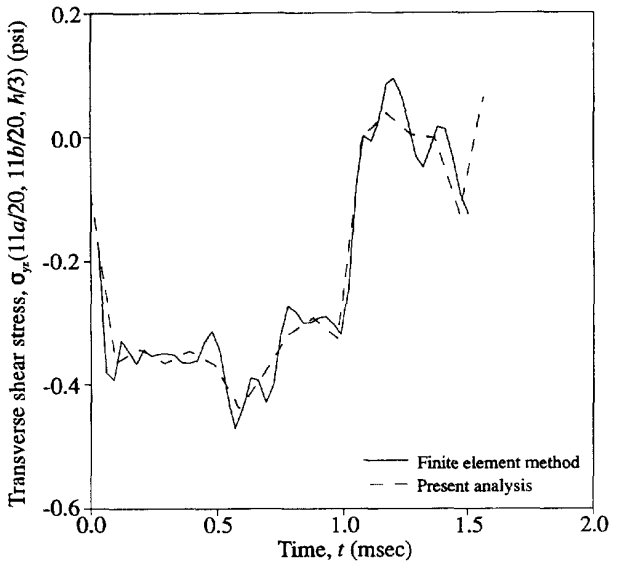

Fig. 8. Variation of transverse shear stress, σ_{yz}, as a function of time for the thin laminate at $x = 11a/20$, $y = 11b/20$, and $z = h/3$.

$$g(x,y) = -100(x-4)^2(x-6)^2(y-4)^2(y-6)^2; \quad 4 \leqslant x \leqslant 6, \quad 4 \leqslant y \leqslant 6 \tag{62}$$

and

$$h(t) = \begin{cases} 1; & t \leqslant 0.001 \text{ s} \\ 0; & t > 0.001 \text{ s} \end{cases}. \tag{63}$$

While the face sheets are free of damping, two different damping parameters, 0.025 and 0.1, are considered for the core. A numerical inverse fast Fourier transform is applied with 16,384 points over time periods of 1.0 and 0.8 second for the lightly and heavily damped cases, respectively. Again, the panel's vibrations attenuate within the specified time periods.

The displacement of a point located beneath the loading surface at the core/face sheet interface ($x = 5.5$, $y = 5.5$, and $z = 0.04$) versus time is presented in Fig. 9. The results reveal that the stress and displacement fields are highly dependent upon the amount of damping used in the analysis. However, the peak magnitudes of the displacement and stress components are not sensitive. The displacement of the panel with a lightly damped core oscillates at a higher frequency than the panel with a damping parameter of 0.1. The normal stresses σ_{xx} and σ_{yy} respond in a manner comparable with the stresses in the lightly damped panel preceding the heavily damped panel as displayed in Figs 10 and 11. The in-plane and transverse shear stresses are observed in Figs 12–14 to respond in a manner consistent with the overall bending of the plate.

5. CONCLUSIONS

In order to predict damage due to an impact, this analysis provides a three-dimensional analytical solution for the stress and displacement fields under specified surface loading resulting from transverse impact. A multi-layer rectangular panel consisting of elastic, homogeneous, and specially orthotropic layers is supported by rollers and is subjected to an arbitrary transverse loading distribution. The governing equations derived from Reissner's functional are solved by applying the Fourier or Laplace transformation in time while enforcing the continuity of tractions and displacements. In this manner, the stress and displacement fields required for damage characterization are determined analytically.

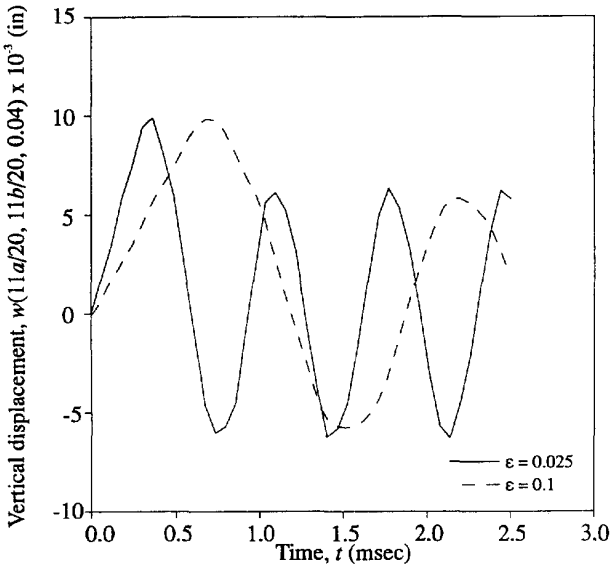

Fig. 9. Variation of vertical displacement, w, as a function of time for the sandwich panel.

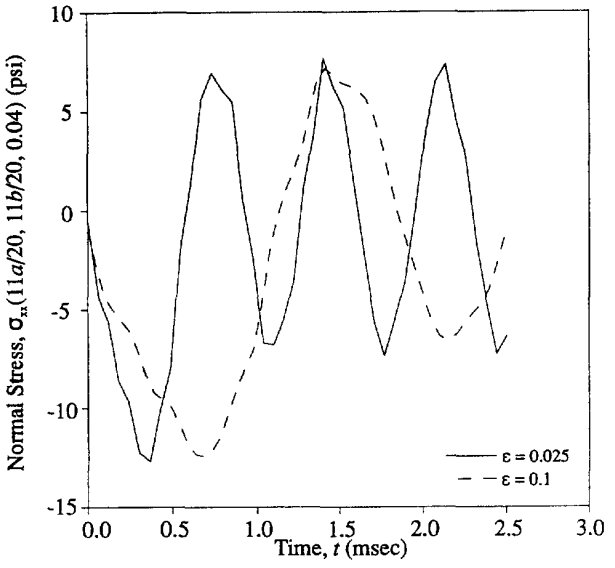

Fig. 10. Variation of normal stress, σ_{xx}, as a function of time for the sandwich panel.

The present solution method was verified by comparing the static results from this analysis with those provided by Pagano (1970). The comparison yields remarkable agreement between this analysis and Pagano's solution and demonstrates the CLT's inability to accurately model relatively thick laminates.

The finite element method was used to construct the transient solution of a thin multilayer panel subject to a transverse loading distribution. The transverse displacement results of the inverse Fourier and inverse Laplace transformations were compared with the results of the finite element analysis and are in favorable agreement. Because the plate elements used in the finite element analysis are incapable of determining the transverse normal stress, this quantity could not be compared.

This analysis provides the basis for many future investigations. The impact analysis and contact phenomenon can be coupled by incorporating the methods introduced by Singh and Paul (1974). This method is an iterative procedure that simultaneously determines the unknown contact area and loading distribution. In this manner, the need for an artificial

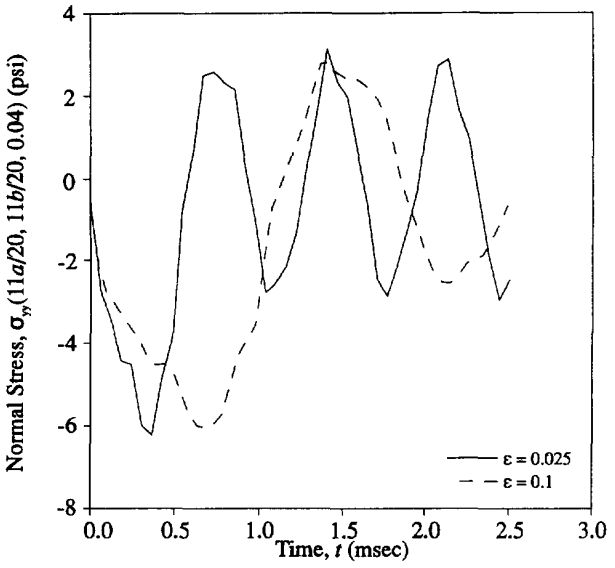

Fig. 11. Variation of normal stress, σ_{yy}, as a function of time for the sandwich panel.

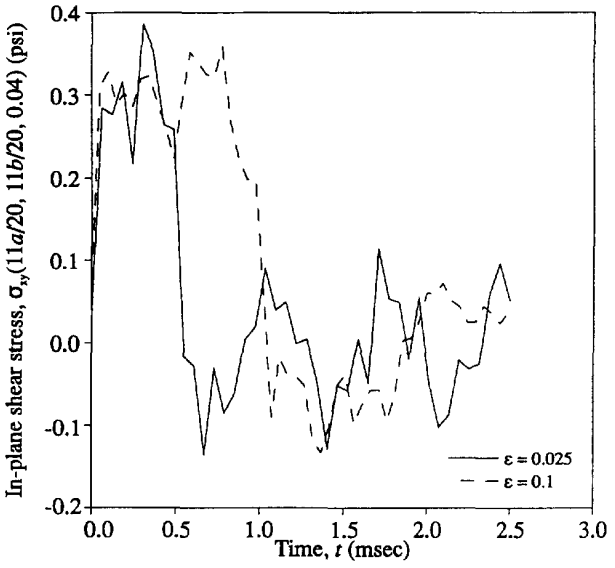

Fig. 12. Variation of in-plane shear stress, σ_{xy}, as a function of time for the sandwich panel.

loading distribution, such as Hertzian loading, is eliminated. With the three-dimensional analytical transient solution for an impacted panel, various damage criteria can then be used to evaluate the structural integrity of the laminate.

The most important subject that needs to be addressed in the future is material damping. In the thin laminate analysis, the damping parameter ε is treated as if small, giving an essentially elastic solution. The sandwich panel analysis, however, contained elastic face sheets without damping laminated to a core with damping. As demonstrated by the response of the sandwich panel, the stress and displacement fields are highly dependent upon the damping factor.

Acknowledgements—This research was conducted under a grant to The University of Arizona from Lockheed Martin Skunk Works.

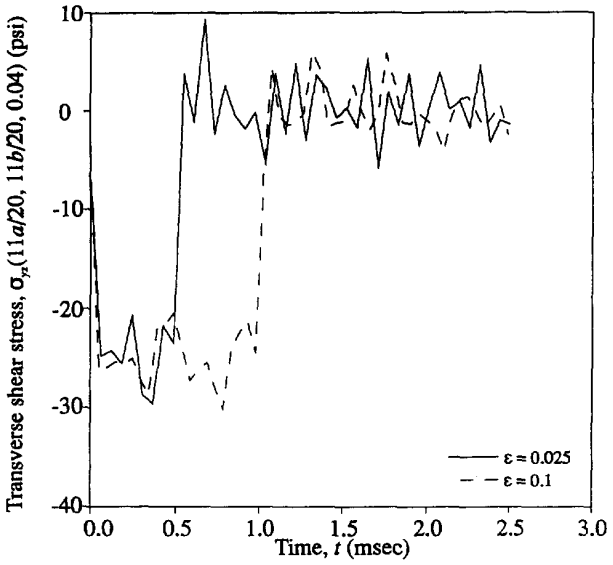

Fig. 13. Variation of transverse shear stress, σ_{xz}, as a function of time for the sandwich panel.

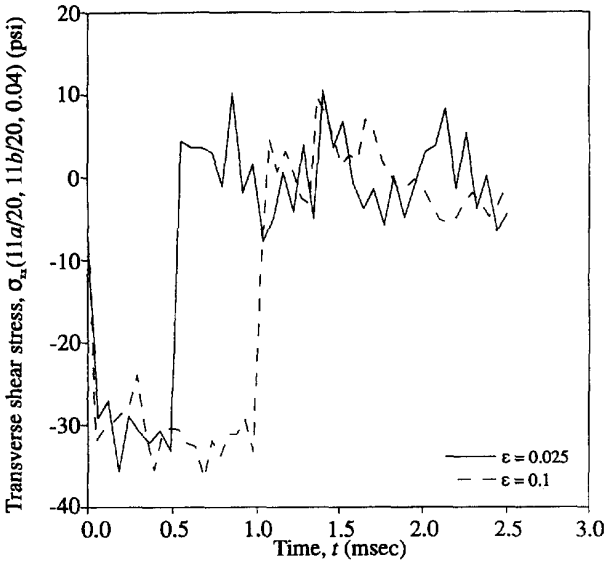

Fig. 14. Variation of transverse shear stress, σ_{xz}, as a function of time for the sandwich panel.

REFERENCES

Ambartsumyan, S. A. (1962) Contributions of the theory of anisotropic layered shells. *Applied Mechanics Review* **15**(4), 245–249.

Cairns, D. S. and Lagace, P. A. (1987) Thick composite plates subjected to lateral loadings. *Journal of Applied Mechanics* **54**, 611–616.

Cairns, D. S. and Lagace, P. A. (1989) Transient response of graphite/epoxy and kevlar/epoxy laminates subjected to impact. *AIAA Journal* **27**(11), 1590–1596.

Chattopadhyay, S. (1977) Response of elastic plates to impact including the effect of shear deformation. In *Proceedings of the 14th Annual Meeting of the Society of Engineering Science, Inc.* ed. G. C. Sih. Lehigh University, Bethlehem, PA, pp. 127–138.

Dobyns, A. L. (1981) Analysis of simply-supported orthotropic plates subject to static and dynamic loads. *AIAA Journal* **19**(5), 642–650.

Dong, S. B., Pister, K. S. and Taylor, R. L. (1962) On the theory of laminated anisotropic shells and plates. *Journal of the Aerospace Sciences* **29**(8), 969–975.

Lee, J. D., Du, S. and Liebowitz, H. (1984) Three-dimensional finite element and dynamic analysis of composite laminate subjected to impact. *Computers and Structures* **19**, 807–813.

Lee, L. J., Huang, K. Y. and Fann, Y. J. (1993) Dynamic responses of composite sandwich plate impacted by a rigid ball. *Journal of Composite Materials* **27**(13), 1238–1256.

Lih, S.-S. and Mal, A. K. (1995) Elastic waves from a distributed surface source in a unidirectional composite laminate. *Impact, Waves and Fracture* eds. R. C. Batra, A. K. Mal and G. P. MacSithigh. AMD-Vol. 205, ASME, New York, pp. 209–219.
Mal, A. K. and Lih, S.-S. (1992) Elastodynamic response of a unidirectional composite laminate to concentrated surface loads: part 1. *Journal of Applied Mechanics* **59,** 878–892.
Mal, A. K. (1988) Wave propagation in layered composite laminates under periodic surface loads. *Wave Motion* **10,** 257–266.
Mindlin, R. D. (1951) Influence of rotary inertia and shear on flexural motions of isotropic, elastic plates. *Journal of Applied Mechanics* **18,** 31–38.
Nettles, A. T., Lance, D. G. and Hodge, A. J. (1990) An examination of impact damage in glass/phenolic and aluminum honeycomb core composite panels. NASA Technical Paper 3042.
Noor, A. K. and Burton, S. B (1990a) Assessment of computational models for multilayered composite shells. *Applied Mechanics Review* **43**(4), 67–97.
Noor, A. K. and Burton, W. S. (1990b) Three-dimensional solutions for antisymmetrically laminated anisotropic plates. *ASME Journal of Applied Mechanics* **57,** 182–188.
Olsson, R. (1992) Impact response of orthotropic composite plates predicted from a one-parameter differential equation. *AIAA Journal* **30**(6), 1587–1596.
Pagano, N. J. (1970) Exact solutions for rectangular bidirectional composites and sandwich plates. *Journal of Composite Materials* **4,** 20–34.
Pister, K. S. and Dong, S. B. (1959) Elastic bending of layered plates. *Journal of the Engineering Mechanics Division, Proceedings of the American Society of Civil Engineers* **EM4,** 1–10.
Ramkumar, R. L. and Chen, P. C. (1983) Low-velocity impact response of laminated plates. *AIAA Journal* **21**(10), 1448–1452.
Reissner, E. and Stavsky, Y. (1961) Bending and stretching of certain types of heterogeneous aeolotropic elastic plates. *Journal of Applied Mechanics* **28,** 402–408.
Reissner, E. (1950) On a variational theorem in elasticity. *Journal of Mathematics and Physics* **24,** 90–95.
Singh, K. P. and Paul, B. (1974) Numerical solution of non-hertzian elastic contact problems. *Journal of Applied Mechanics* **41** 484–490.
Starnes, J. H., Jr. and Williams, J. G. (1984) Failure characteristics of graphite/epoxy structural components loaded in compression. NASA TM-84552.
Whitney, J. M. and Sun, C.-T. (1977) Transient response of laminated composite plates subjected to transverse dynamic loading. *Journal of the Acoustical Society of America* **61**(1), 101–104.
Wu, H.-S. T. and Springer, G. S. (1988) Impact induced stresses, strains, and delaminations in composite plates. *Journal of Composite Materials* **22,** 533–560.

APPENDIX: AVERAGE MATERIAL CONSTANTS FOR BALANCED LAMINATES

Since only specially orthotropic materials can be examined using this formulation, laminates with plies oriented at other than 0° or 90° cannot be analyzed. A method exists, however, that determines the average specially orthotropic stiffness matrix for a balanced laminate. A balanced laminate is a panel that has a negatively oriented ply for every positively oriented ply. For example, for every $+35°$ ply there is a $-35°$ ply. Thus, this analysis can be expanded to model any balanced laminate if an average stiffness or compliance matrix is determined.

To determine the average stiffness matrix, the stiffness matrix of each ply in the global coordinates is required. The stress–strain relationship for the kth layer of a laminate can be represented as

$$\boldsymbol{\sigma}^k = \mathbf{C}^k \boldsymbol{\varepsilon}^k \tag{A1}$$

or

$$\tilde{\boldsymbol{\sigma}}^k = \tilde{\mathbf{C}}^k \tilde{\boldsymbol{\varepsilon}}^k \tag{A2}$$

where the "~" denotes the quantities in the local reference frame. The unit vectors of the local reference frame can be written in terms of the direction cosines and the global unit vectors as

$$\begin{Bmatrix} \mathbf{n}_\xi \\ \mathbf{n}_\eta \\ \mathbf{n}_\zeta \end{Bmatrix}^k = \begin{bmatrix} l_1 & m_1 & n_1 \\ l_2 & m_2 & n_2 \\ l_3 & m_3 & n_3 \end{bmatrix}^k \begin{Bmatrix} \mathbf{n}_x \\ \mathbf{n}_y \\ \mathbf{n}_z \end{Bmatrix}. \tag{A3}$$

With these direction cosines, stresses and strains can be transformed to the global reference frame through the transformation

$$\boldsymbol{\sigma}^k = \mathbf{T}^k \tilde{\boldsymbol{\sigma}}^k$$
$$\boldsymbol{\varepsilon}^k = \mathbf{T}^k \tilde{\boldsymbol{\varepsilon}}^k \tag{A4}$$

where

$$\mathbf{T}^k = \begin{bmatrix} l_1^2 & l_2^2 & l_3^2 & 2l_2l_3 & 2l_1l_3 & 2l_1l_2 \\ m_1^2 & m_2^2 & m_3^2 & 2m_2m_3 & 2m_1m_3 & 2m_1m_2 \\ n_1^2 & n_2^2 & n_3^2 & 2n_2n_3 & 2n_1n_3 & 2n_1n_2 \\ m_1n_1 & m_2n_2 & m_3n_3 & (m_2n_3+m_3n_2) & (m_1n_3+m_3n_1) & (m_1n_2+m_2n_1) \\ l_1n_1 & l_2n_2 & l_3n_3 & (l_2n_3+l_3n_2) & (l_1n_3+l_3n_1) & (l_1n_2+l_2n_1) \\ l_1m_1 & l_2m_2 & l_3m_3 & (l_2m_3+l_3m_2) & (l_1m_3+l_3m_1) & (l_1m_2+l_2m_1) \end{bmatrix}. \tag{A5}$$

Substituting eqns (A3) and (A4) into (A1) while noting that

$$\mathbf{T}^k\mathbf{T}^{k^{-1}} = \mathbf{I} \tag{A6}$$

yields

$$\boldsymbol{\sigma}^k = \mathbf{T}^k\bar{\mathbf{C}}^k\mathbf{T}^{k^T}\boldsymbol{\varepsilon}^k. \tag{A7}$$

Thus, the transformation of the stiffness matrix from local coordinates to global coordinates is

$$\mathbf{C}^k = \mathbf{T}^k\bar{\mathbf{C}}^k\mathbf{T}^{k^T}. \tag{A8}$$

The average stiffness matrix, $\mathbf{C}$, of a balanced laminate is then represented by

$$\mathbf{C} = \frac{1}{h}\sum_1^n \mathbf{t}^k\mathbf{C}^k \tag{A9}$$

which represents an average weighting of the stiffness matrix based on the thickness of the layer. Provided the laminate is balanced, $\mathbf{C}$ will represent a specially orthotropic material with 12 nonzero coefficients, 9 of which are independent. This averaging process is expected to provide reasonably acceptable results, provided the paired balancing plies are located closely to one another and the plies are relatively thin.